Optimized optical phase conjugation configuration for fiber nonlinearity compensation in CO-OFDM systems

Lujiao Li (李炉焦), Yaojun Qiao (乔耀军)*, and Yuefeng Ji (纪越峰)

Key Laboratory of Information Photonics and Optical Communications, Ministry of Education, Beijing University of Posts and Telecommunications, Beijing 100876, China.

**Corresponding author: qiao@bupt.edu.cn*

Received November 29, 2010; accepted January 28, 2011; posted online May 12, 2011

The optimized optical phase conjugation (OPC) configuration is proposed for the 40-Gb/s CO-OFDM system. The proposed configuration for nonlinear cancellation is systematically depicted in transmission links with lumped amplification. Numerical simulations are performed to demonstrate effectiveness. Simulation results show that mid-span spectral inversion (MSSI) can partially compensate for nonlinear distortions. Moreover, its optimized configuration can further improve system performances and increase nonlinear compensation effectiveness. Compared with MSSI, the maximal Q factor, nonlinear threshold, and transmission distance of optimized OPC configuration increase by over 1.6 dB, 2 dB, and 2 times, respectively.

OCIS codes: 060.2330, 060.4370, 190.3270, 190.5040.
doi: 10.3788/COL201109.060604.

Coherent optical orthogonal frequency division multiplexing (CO-OFDM) for long haul and high speed transmission has attracted significant attention[1,2] due to its high spectral efficiency and robust tolerance to linear impairments, such as chromatic dispersion and polarization mode dispersion[3,4]. However, optical OFDM is highly susceptible to fiber nonlinearity. Several methods have already been proposed to compensate for nonlinear impairment[5,6], but they are relatively complicated.

The optical phase conjugation (OPC) technology was proposed by Yariv *et al.* in 1979 to compensate for chromatic dispersion[7]. Since then, OPC has been widely used to compensate for nonlinear distortions resulting from the Kerr effect, such as self phase modulation (SPM), intrachannel nonlinear effects, and nonlinear phase noise[8]. Simultaneous compensation of nonlinear effects and chromatic dispersion by the OPC has also been shown in Ref. [9]. All these applications of OPC are in a single carrier system. Recently, OPC has been used in OFDM system[10,11]. Theoretically, mid-span spectral inversion (MSSI) can effectively cancel nonlinearity for transmission links with symmetrical power profile. However, this condition cannot be satisfied in transmission links using lumped amplification, thus limiting effectiveness of nonlinearity cancellation of MSSI.

In this letter, we propose an optimized OPC configuration to increase nonlinearity compensation effectiveness of the OPC in 40-Gb/s CO-OFDM system. A specific amount of fiber is applied to produce symmetrical nonlinear regions distribution with respect to zero accumulated dispersion. Simulations show that the optimized configuration is highly effective in suppressing nonlinear distortions in 40-Gb/s CO-OFDM system.

Recently, Watanabe *et al.*[9] proposed the conditions for exact compensation of both chromatic dispersion and Kerr effect by OPC as follows:

$$D_{s1}L_1 = D_{s2}L_2, \tag{1}$$

$$\gamma_1\overline{P_1}L_1 = \gamma_2\overline{P_2}L_2, \tag{2}$$

where D_{sj} (j=1, 2) is the dispersion parameter of standard single-mode fiber (SSMF) of fiber-j (fiber-1 is the first fiber placed before OPC and fiber-2 is the second fiber placed after OPC, as shown in Fig. 1(a)), L_j is the length of fiber-j, γ_j is the nonlinearity coefficient of fiber-j, and $\overline{P_j}$ is the path-averaged optical power, where $\overline{P_1} = \left[\int_{-L_1}^{0} P_1(z)\mathrm{d}z\right]/L_1$ and $\overline{P_2} = \left[\int_{0}^{L_2} P_2(z)\mathrm{d}z\right]/L_2$ and P_j is the optical power in fiber-j. Equations (1) and (2) indicate the dispersion and nonlinearity compensation conditions, respectively[9]. However, satisfying the two conditions in transmission links with odd-span fiber, lump amplification, and MSSI is difficult. An example of three-span (SSMF A, B, and C, OPC is placed after A) is shown in Fig. 1(a). The number of fiber spans, erbium-doped fiber amplifiers (EDFAs), and the nonlinear regions before OPC are different from those after OPC. Nonlinear regions are link regions where nonlinear effects become important for pulse evolution. This corresponds to the nonlinear effective length L_{eff} and rectangles in Fig. 1. Consequently, it is hard to satisfy

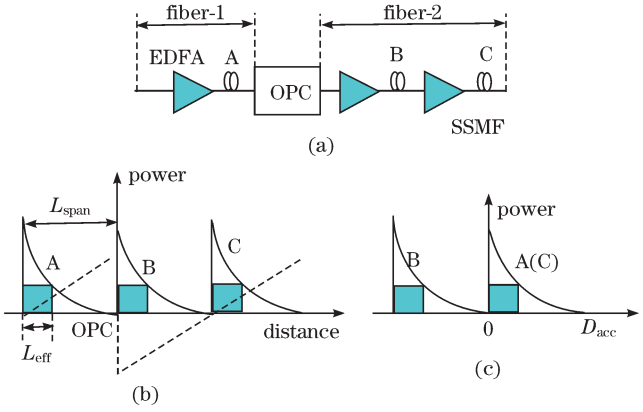

Fig. 1. (a) Odd-span transmission link with MSSI; (b) asymmetrical power profiles with respect to the OPC caused by periodic lump amplification, dashed line shows accumulated dispersion distribution along the link; (c) asymmetrical nonlinear regions distribution with respect to zero accumulated dispersion D_{acc}.

Eqs. (1) and (2), and power profiles are asymmetrical with respect to the position of OPC (Fig. 1(b)). Simultaneously, nonlinear region distribution is asymmetrical with respect to zero accumulated dispersion (Fig. 1(c)). Thus, nonlinearity in this system cannot be cancelled effectively.

To improve OPC effectiveness, we optimized the OPC configuration by adding EDFA and a specific amount of fiber. An example is shown in Fig. 2(a). The OPC subsystem of the optimized OPC configuration contains an added EDFA, added fiber, and the conventional OPC. At the same time, another EDFA and fiber are added at the receiver. The optimization of the OPC configuration and the characteristics of the added fiber are based on the following two hypotheses.

Hypothesis-1: the number of nonlinear regions before OPC is similar to that after the OPC. Hypothesis-2: nonlinear regions are symmetrical with respect to a certain object. Due to the difficulty in fulfilling the condition where nonlinear regions are symmetrical with respect to OPC in transmission links with lump amplification, another object has to be considered. To simultaneously suppress nonlinearity and chromatic dispersion, nonlinearity must be totally cancelled at zero accumulated dispersion after the OPC. Thus, considering the nonlinear regions as symmetrical with respect to zero accumulated dispersion is helpful. This was also adopted by Minzioni *et al.*[17]. This hypothesis (hypothesis-2), is the most important condition to compensate for nonlinear distortions.

In a transmission link with different spans of uniform fiber before and after the OPC of the MSSI, there are two cases where the OPC can be placed. Case (i): the numbers of fiber spans of fiber-1 and fiber-2 are N-1 and N (N: positive integer), respectively. An example is shown in Fig. 2(a). Case (ii): the numbers of fiber spans of fiber-1 and fiber-2 are N and N-1, respectively, as shown in Fig. 3(a). In these links, we added the proper length of fiber to satisfy the two hypotheses discussed earlier.

In case (i), a length $L_{\rm span}$ of the added fiber of the OPC subsystem ($L_{\rm span}$ is the length of one-span fiber), and the added fiber has the same characteristics as the transmission fiber which can satisfy the conditions of Eqs. (1) and (2). Simultaneously, hypothesis-1 is likewise satisfied.

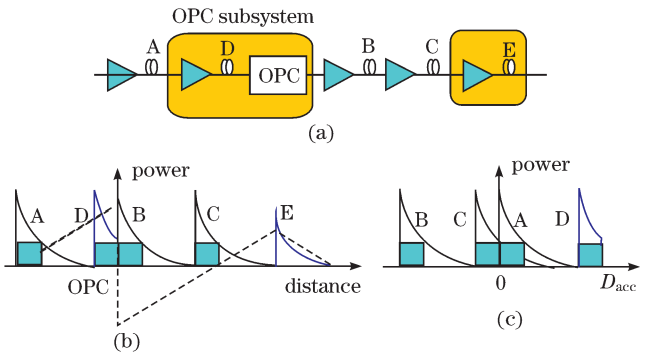

Fig. 2. (a) Transmission link of case (i) with optimized OPC configuration; (b) asymmetrical power profiles with respect to the OPC, dashed line shows accumulated dispersion distribution along the link; (c) symmetrical nonlinear regions distribution with respect to zero accumulated dispersion $D_{\rm acc}$.

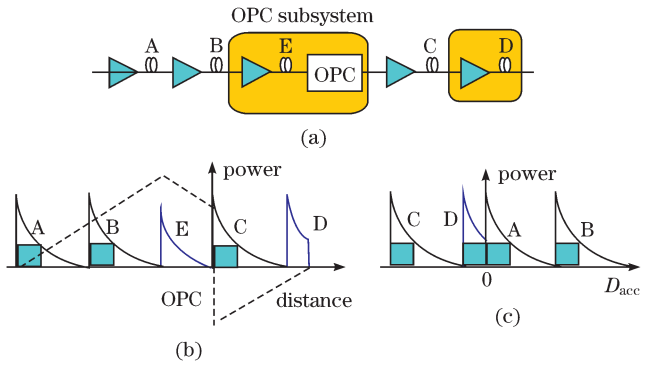

Fig. 3. (a) Transmission link of case (ii) with optimized OPC configuration; (b) asymmetrical power profiles with respect to the OPC, dashed line shows accumulated dispersion distribution along the link; (c) symmetrical nonlinear regions distribution with respect to zero accumulated dispersion $D_{\rm acc}$.

However, hypothesis-2 cannot be satisfied in this way, and a fiber of one-span length is impractical and wasteful. Therefore, an optimal fiber length rather than one-span should be considered. The nonlinear regions of fiber-2 are larger by one than that of fiber-1, and one nonlinear region corresponds to the nonlinear effective length $L_{\rm eff}$. Therefore, we added a fiber of length $L_{\rm eff}$. A similar length was used in Ref. [12]. In Fig. 2(a), an EDFA and a SSMF D of length $L_{\rm eff}$ are added immediately before OPC to build the OPC subsystem. Subsequently, the dispersion of fiber-1 is compensated to zero at the $L_{\rm eff}$ of fiber C by the OPC subsystem (Fig. 2(b)). The nonlinear regions become symmetrical with respect to zero accumulated dispersion (Fig. 2(c)). Moreover, a certain length of dispersion compensation fiber (DCF) E (its nonlinearity is ignored) at the receiver is used to eliminate residual dispersion. This is called optimized OPC configuration optimized-OPC-1. The identical optimization setup of the OPC is obtained from Ref. [12]. However, the study considers only case (i). Thus, we investigated the optimization of OPC in case (ii).

In case (ii), a three-span transmission link is taken as an example, in which the OPC is placed after fiber B (Fig. 3(a)). To satisfy hypothesis-1, a nonlinear region must be added to fiber-2, which can be achieved by adding a SSMF D of length $L_{\rm eff}$ at the receiver. This is not the case with hypothesis-2. Considering that dispersion of $D_{\rm s}(L_{\rm span}-L_{\rm eff})$ before the OPC cannot be compensated for, a linear DCF E with dispersion of $-D_{\rm s}(L_{\rm span}-L_{\rm eff})$ is added immediately before the OPC to build the OPC subsystem. Nonlinearity of this added fiber is ignored because it will add a nonlinear region and leads to different nonlinear regions before and after the OPC. Consequently, the residual dispersion is zero after fiber D as shown in Fig. 3(b). Figure 3(c) shows that nonlinear regions are symmetrical with respect to zero accumulated dispersion $D_{\rm acc}$. Eventually, hypothesis-1, hypothesis-2, and Eqs. (1) and (2) are simultaneously satisfied. Likewise, the DCF E can be replaced with a SSMF of dispersion $D_{\rm s}(L_{\rm span}-L_{\rm eff})$ (its nonlinearity is also ignored) immediately after the OPC to meet the four conditions. This optimized OPC configuration is named optimized-OPC-2. Comparing the optimized OPC configuration of case (ii) with that of case (i), the added SSMF D

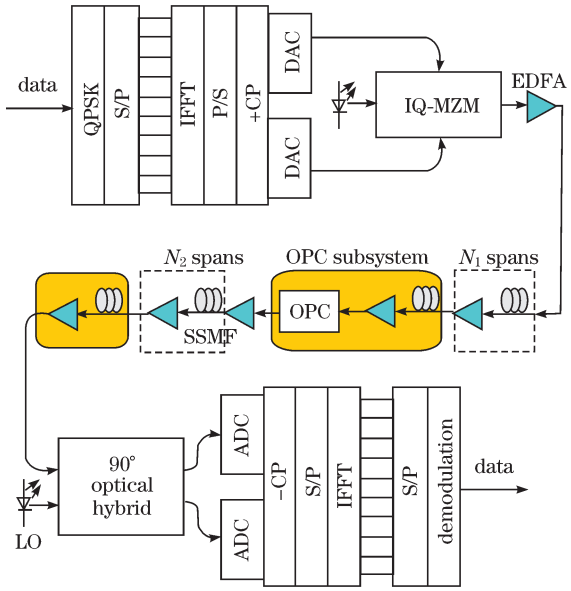

Fig. 4. Simulation configuration.

of length L_{eff}, aimed at adding a nonlinear region is placed at the receiver, and the added linear fiber E is included in the OPC subsystem in case (ii), these are contrary to case (i). The performance of MSSI and optimized-OPC in the two cases are compared. Maximal Q factor of case (ii) is higher than that of case (i). These are explained as follows. In case (ii), the number of span of fiber-1 is larger by one than that of fiber-2. After OPC, a large negative chromatic dispersion acted as pre-compensation dispersion for fiber-2, whereas a small dispersion was observed in case (i). Thus, SPM effect is weaker in case (ii) than in case (i); case (ii) has a better performance than case (i).

For a comprehensive analysis, the even-span link is considered. In an even-span transmission link applying MSSI, uniform fiber, and identical optical power before and after the OPC, the same number of fiber spans and EDFAs exists. And the transmission link has the same path-averaged optical power before and after the OPC.

Consequently, hypothesis-1 and Eqs. (1) and (2) are satisfied, but not hypothesis-2. Since the number of nonlinear regions of fiber-1 is identical to that of fiber-2, only the addition of linear fiber is required to satisfy hypothesis-2. Based on the discussions on odd-span, the length of the added fiber of the OPC subsystem is easy to obtain. When a SSMF is added immediately after the OPC, its length is $L_{\text{span}} - L_{\text{eff}}$, whereas if a DCF is added immediately before the OPC, its length is $-D_{\text{s}}(L_{\text{span}} - L_{\text{eff}})/D_{\text{c}}$, where D_{c} is the dispersion parameter of DCF. At the receiver, an appropriate length of another added DCF is used to compensate for residual dispersion. The condition of hypothesis-2 is fulfilled. A similar setup was reported in Ref. [12]. In this letter, it is called optimized configuration of the OPC optimized-OPC-3.

To test the optimized OPC configuration, numerical simulations were performed in a 40-Gb/s CO-OFDM system. VPIsystems' VPItransmissionMaker V7.6 was used for simulations, and the schematic of this system was shown in Fig. 4. The original data are first mapped on 1,024 frequency subcarriers with quardrature phase shift keying (QPSK) modulation format, and subsequently transferred to the time domain by an inverse fast Fourier transform (IFFT) with the size of 2,048 with a zero padding ratio of 50%. A cyclic prefix (CP) of length 256 is used. The resulting electrical OFDM data signal is then electro-optically converted using an IQ Mach-Zehnder modulator (IQ-MZM). The transmission link consists of N_1 and N_2 spans of 80-km SSMF before and after the OPC subsystem, respectively. The OPC subsystem is composed of the conventional OPC, an added EDFA, and an added fiber. Another EDFA and fiber are also added at the receiver to optimize OPC configuration. All the added EDFAs and fibers are shown in the gold-colored region of Fig. 4. The parameters of SSMF are fiber loss $\alpha = 0.2$ dB/km, dispersion coefficient $D_{\text{s}} = 16$ ps/(nm·km), dispersion slope of 0.08 ps/(nm^2·km), and nonlinearity coefficient $\gamma = 1.3$ W^{-1}·km^{-1}. The parameters of DCF are fiber loss $\alpha = 0.5$ dB/km and dispersion coefficient $D_{\text{c}} = -90$ ps/(nm·km). The loss of SSMF in each span is compensated by an EDFA. The EDFA, with 6-dB noise figure, is also used to control the SSMF launch power. At the optical receiver, the OFDM signal beats with the local oscillator (LO) signal in an optical 90° hybrid to obtain the I and Q components of the signal. The transmitter laser and the LO have a 100-kHz line width and set to have zero frequency offset. After hard decision and decoding, the bit-error-rate (BER) is investigated.

A transmission of 1,520 km (19 spans) was investigated. The optimal length of the added SSMF for optimized OPC configuration in case (ii) was tested. The Q factor as a function of the length at input power $P_{\text{in}} = 6$ dBm is shown in Fig. 5. The Q factor reaches its maximum value when the length is close to 21 km. On the other hand, according to the above theory analysis, the length of the added SSMF is $L_{\text{eff}} = 21$ km, indicating a good agreement between simulation and theory analysis. In the following simulations, the length of 21 km was used.

Figure 6 shows the received constellation diagrams after 1,520-km transmission in case (i) without OPC at $P_{\text{in}} = 3$ dBm and with OPC (including MSSI and optimized OPC configuration) at $P_{\text{in}} = 6$ dBm. For the system without OPC, the performance degradation and the corresponding Q factor is 8.5 dB. When the MSSI is used, the constellation diagram opens and the corresponding Q factor is 12.8 dB, indicating efficient performance improvement. Moreover, optimized OPC configuration provided further improvement, which subsequently separated constellation points. The corresponding Q factor is 19.0 dB.

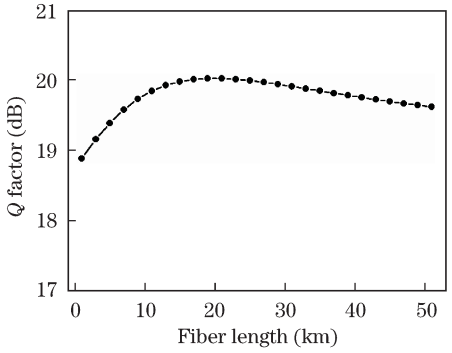

Fig. 5. Q factor versus length of the added SSMF.

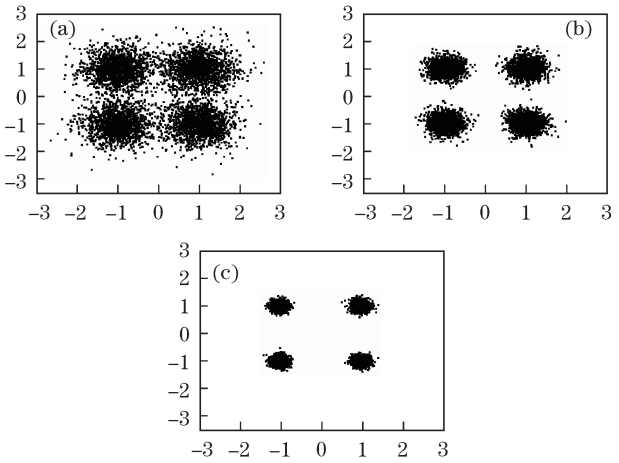

Fig. 6. Constellation diagrams after 1,520-km transmission (a) without OPC at $P_{\rm in} = 3$ dBm, (b) with the MSSI, and (c) with optimized OPC configuration at $P_{\rm in} = 6$ dBm.

Figure 7 shows the Q factor performance as a function of input power with and without the OPC for transmission reach of 19 spans. The MSSI-1 and optimized-OPC-1 correspond to MSSI of case (i) and its optimized configuration, respectively. The MSSI-2 and optimized-OPC-2 are the corresponding setup of case (ii). The figure shows a similar performance at low input power. However, a significant difference for high input power is observed. The MSSI and optimized-OPC can partially and significantly improve the Q factor performance. The maximal Q factor increased by about 2.3 and 2.7 dB with the application of MSSI to cases (i) and (ii) respectively. The factor further increased by 1.6 and 2.2 dB for cases (i) and (ii) by optimizing OPC configuration. The nonlinear threshold (NLT) was used as a performance metric to estimate the susceptibility of a system to nonlinear effects. In this letter, this is defined as the launch power at which point Q reaches the forward error correction (FEC) threshold, which is 9.2 dB (or BER of 2×10^{-3}). In Fig. 7, NLT increased by over 5 dB when the MSSI is used. After optimizing OPC configuration, the NLT further increased by more than 2 dB for both cases (i) and (ii). Therefore, the optimized-OPC can strongly improve performance and effectiveness of the MSSI. Figure 7 also shows that the performance of the MSSI-1 is worse than that of the MSSI-2 for input power < 4 dBm, which is contrary to input power > 4 dBm.

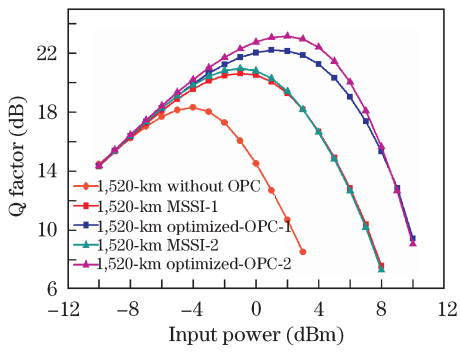

Fig. 7. Q factor versus input power after 1,520-km transmission with MSSI, with optimized OPC configuration, and without the OPC.

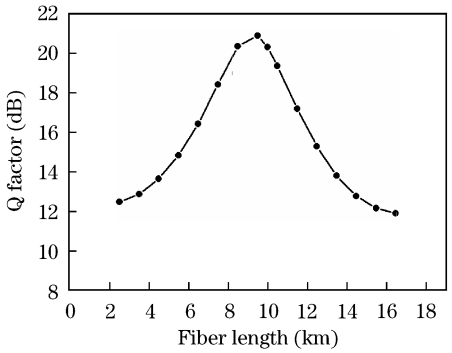

Fig. 8. Q factor versus the length of the added fiber of the OPC subsystem.

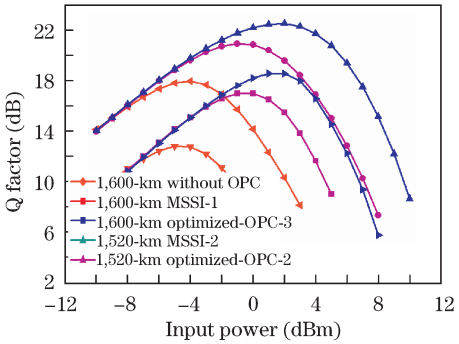

Fig. 9. Q factor versus input power for 40-Gb/s CO-OFDM transmission with the MSSI, with the optimized-OPC-3, and without the OPC.

The same trend is observed when comparing the optimized-OPC-1 with the optimized-OPC-2 where the turning point is 9 dBm. These indicate that at low input power (< 4 dBm for MSSI and < 9 dBm for optimized-OPC), the application of OPC (MSSI and optimized-OPC) to case (ii) facilitates better performance than when it is applied to case (i). Moreover, the maximal Q factor of the MSSI-2 (the optimized-OPC-2) is 0.3 dB (1 dB) higher than that of the MSSI-1 (the optimized-OPC-1). Thus, the optimized OPC configuration in case (ii) is the better choice when an optimum launch power is used.

Even-span transmission link was simulated as well. According to the above analysis, a DCF, placed immediately before the OPC, of length $-D_{\rm s}(L_{\rm span} - L_{\rm eff})/D_{\rm c}$ was added to the OPC subsystem to optimize the OPC configuration. With given parameters of $L_{\rm span} = 80$ km, $L_{\rm eff} = 21$ km, we determined the length of this DCF to be approximately 10.5 km. On the other hand, the optimal length of this DCF was investigated through simulation. The Q factor as a function of the length at a transmission of 1,600 km and $P_{\rm in} = 6$ dBm is shown in Fig. 8. The maximum Q is obtained when the length is about 9.5 km, which agrees well with the theory analysis. The length of 10.5 km was adopted in the following simulations.

We compared the proposed configuration with the MSSI and the link without the OPC at transmission distances of 1,600 and 4,800 km. Figure 9 shows the Q performance as a function of input power. As launch power increases, the system becomes limited by nonlinear distortions. A significant increase of Q factor is

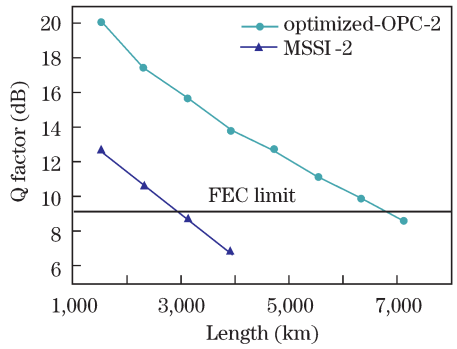

Fig. 10. Q factor versus transmission distance with the MSSI and with optimized OPC configuration of case (ii) at $P_{\rm in} = 6$ dBm.

observed with the MSSI. Moreover, further improvement is observed when comparing the optimized-OPC-3 with MSSI. When the MSSI is adopted, the maximal Q factor increased by ∼3 and > 4 dB for transmission lengths of 1,600 and 4,800 km, respectively. An additional 1.6-dB improvement is obtained for both transmission lengths of 1,600 and 4,800 km when the optimized OPC configuration is applied. In Fig. 9, NLT apparently increases by more than 5 dB when the MSSI is used for both transmission distances of 1,600 and 4,800 km. Moreover, the NLT further improved by over 2 dB through optimizing OPC configuration. Therefore, MSSI can partially compensate for nonlinearity. Moreover, nonlinearity can be effectively compensated by the optimized OPC configuration. This indicates that the optimized-OPC-3 can significantly increase the effectiveness of MSSI, and consequently improve system performance.

Figure 10 shows the Q factor as a function of the transmission distance at $P_{\rm in} = 6$ dBm for case (ii). With MSSI, the Q factor is below 9.2 dB after 3,120-km transmission. When optimized OPC configuration is applied, the maximum transmission distance of 6,320 km is feasible with a Q factor over the FEC limit. This corresponds to an increase in transmission length by over 2 times. The increase of the transmission distance by the optimized OPC configuration for case (i) and even-span transmission is also simulated, and the results are almost similar to those of case (ii).

In conclusion, we propose an approach to optimize configuration of the OPC in 40-Gb/s CO-OFDM system, which leads to an increase in the effectiveness of nonlinearity compensation. The optimized OPC configuration in this letter is considered mainly for odd-span transmission, although it is applicable to even-span transmission as well. Simulations show that the optimized configuration outperforms the MSSI in different transmission links. The maximal Q factor, the NLT, and the transmission distance increase by more than 1.6 dB, 2 dB, and 2 times, respectively. Two different configurations in a transmission link with odd-span fiber are compared. Applying the OPC (not only MSSI but also the optimized-OPC) to case (i) shows a slightly better performance than case (ii) in high-nonlinearity system. However, the MSSI and the optimized-OPC in case (ii) show better performance at low input power and higher maximal Q factor.

This work was supported in part by the National Natural Science Foundation of China (No. 60932004), the National "863" Program of China (No. 2009AA01A345), and the National "973" Program of China (No. 2007CB310705).

References

1. Y. Qiao, Z. Wang, and Y. Ji, Chin. Opt. Lett. **8,** 888 (2010).
2. Y. Wu, J. Li, C. Zhao, Y. Zhao, F. Zhang, and Z. Chen, Chin. Opt. Lett. **8,** 634 (2010).
3. H. Takahashi, A. A. Amin, S. L. Jansen, I. Morita, and H. Tanaka, in *Proceedings of OFC 2009* PDPB7 (2009).
4. W. Peng, K. Feng, and S. Chi, Opt. Express **18,** 1916 (2010).
5. L. B. Du and A. J. Lowery, Opt. Express **18,** 17075 (2010).
6. X. Liu and R. W. Tkach, in *Proceedings of OFC 2009* OTuO5 (2009).
7. A. Yariv, D. Fekete, and D. M. Pepper, Opt. Lett. **4,** 52 (1979).
8. S. L. Jansen, D. van den Borne, P. M. Krummrich, S. Spälter, G.-D. Khoe, and H. de Waardt, IEEE J. Sel. Top. Quant. Electron. **12,** 505 (2006).
9. S. Watanabe and M. Shirasaki, J. Lightwave Technol. **14,** 243 (1996).
10. X. Liu, Y. Qiao, and Y. Ji, Opt. Commun. **283,** 2749 (2010).
11. V. Pechenkin and I. J. Fair, J. Opt. Commun. Netw. **2,** 701 (2010).
12. P. Minzioni, F. Alberti, and A. Schiffini, J. Lightwave Technol. **23,** 2364 (2005).